PHASE CHARACTERISTICS OF SOURCE TIME FUNCTION MODELED BY STOCHASTIC IMPULSE TRAIN

H MORIKAWA[1], S SAWADA[2], K TOKI[3], K KAWASAKI[4] And Y KANEKO[5]

SUMMARY

In order to discuss the relationship between the lower and higher frequency components of source spectra, we deal with impulse train model as source time function. Considering the successive rupture of small extent on a fault plane, we represent the source time function by time series which consist of random sequence of impulses. Under this assumption, the spectral characteristics of source time function are obtained analytically and numerically from the stochastic viewpoints: namely, on one hand, the trend of impulse train determines the frequency characteristics of phase spectrum in lower frequency range, and on the other hand, the uctuation from the trend settles higher frequency range. Furthermore, it is shown that the spectral properties of source time function can be determined using only two parameters which are number of impulses N and probability density function (PDF) of occurrence time of impulse $f_T(t)$.

INTRODUCTION

The objective of this study is to discuss the relationship between the lower and higher frequency components of source spectra and to model its spectral properties. For this purpose, we will deal with impulse train model as source time function, because spectral characteristics of source time function depend on the occurrence time of impulse function which corresponds to small extent on the fault. Considering the successive rupture of small extent on a fault plane, we will represent the source time function by impulses which are randomly generated on time axis from a probability model.

There are many studies which deal with the stochastic processes of impulse train. Most of such studies are focused on the problems of \point process," which are mainly discussed as counting problems [ex. Daley and Vere-Jones, 1988]. These studies did not treat the Fourier spectrum, while a few researchers deal with power spectra for spectral representation of the point processes [ex. Vanmarcke, 1983, and Lin and Cai, 1995].

We analytically derive the stochastic properties for Fourier amplitude and phase spectrum of time series which consist of impulses occurred randomly. In particular, introducing the group delay time spectrum $t_{gr}(\omega)$ instead of Fourier phase spectrum, which is the gradient of phase spectrum, the stochastic characteristics of phase in frequency domain will be made clear. While the basic ideas of $t_{gr}(\omega)$ have been appeared more than twenty years ago [Ohsaki, 1979, Izumi and Katsukura, 1983, and Soda, 1986], there were little studies on this problem in this decade. We discuss newly the the group delay time spectrum from the viewpoints of stochastic impulse train.

[1] School of Civil Engineering, Tottori University, Japan, E-mail: morika@mcn.ne.jp
[2] Disaster Prevention Research Inst, Kyoto Univ, Japan,E-mail: sawada@cat_sh.dpri.kyoto-u.ac.jp
[3] Graduate School of Civil Engineering, Kyoto University, Japan,E-mail: toki@quake.kuciv.kyoto-u.ac.jp
[4] Graduate School of Civil Engineering, Kyoto University, Japan,E-mail: toki@quake.kuciv.kyoto-u.ac.jp
[5] Sumitomo Trust & Banking Co., Ltd., Japan, E-mail: y.kaneko@b2.ezweb.ne.jp

2. PROBLEM SETTING

We will treat a time series obtained by

$$x(t) = \sum_{k=1}^{N} \alpha\delta(t - t_k), \tag{1}$$

where $\delta(t)$ is Dirac's delta function, α magnitude of impulses, N number of impulses, and t_k random variable following any probability density function (PDF) $f_T(t)$. It should be noted that the magnitude α can be constant without the loss of generality, because we can consider that some impulses occur at same time t_k in a case where the impulses have different magnitudes.

Using the relation that the Fourier transform of $\delta(t)$ is $\exp[-i\omega]$, where $i = \sqrt{-1}$, and ω is circular frequency, the Fourier transform of $x(t)$ becomes

$$X(\omega) = \alpha \sum_{k=1}^{N} \exp[-i\omega t_k]. \tag{2}$$

Rewriting $X(\omega)$ as $A(\omega)\exp[-i\phi(\omega)]$, the Fourier amplitude $A(\omega)$ and phase spectrum $\phi(\omega)$ yield, respectively,

$$A(\omega) = \alpha \sqrt{\sum_{k=1}^{N}\sum_{\ell=1}^{N} \cos\omega(t_k - t_\ell)} \tag{3}$$

$$\phi(\omega) = \tan^{-1} \frac{\displaystyle\sum_{k=1}^{N} \sin\omega t_k}{\displaystyle\sum_{k=1}^{N} \cos\omega t_k}. \tag{4}$$

Then the group delay time spectrum $t_{gr}(\omega)$ of $x(t)$ is derived as

$$t_{gr}(\omega) = \frac{d\phi(\omega)}{d\omega} = \frac{\displaystyle\sum_{k=1}^{N}\sum_{\ell=1}^{N} t_k \cos\omega(t_k - t_\ell)}{\displaystyle\sum_{k=1}^{N}\sum_{\ell=1}^{N} \cos\omega(t_k - t_\ell)}. \tag{5}$$

To examine the generality of the constant magnitude α, a simple example is presented in Figure 1. The uppermost panel (a) of this figure shows two impulses with different magnitudes, and the other panels compare the results obtained from the Eqs.(3) and Eq.(5) and from fast Fourier transform (FFT) method. Since these figures seem to be same, we can accept the supposition of constant magnitude of impulses.

The binomial variate, generally speaking, is the number of successes in n-independent Bernoulli trials where the probability of success at each trial is p and the probability of failure is $1 - p$. The probability function of the binomial variate X_n is represented by

$$P(X_n = x) = \binom{n}{x} p^x (1-p)^{n-x} \qquad (x = 0, 1, 2, \ldots, n). \tag{6}$$

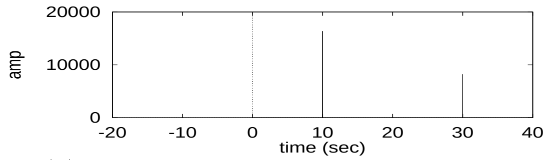

(a) Impulse train with different magnitude

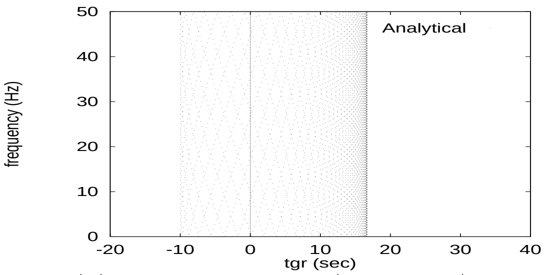

(b) Group delay time (Analytical)

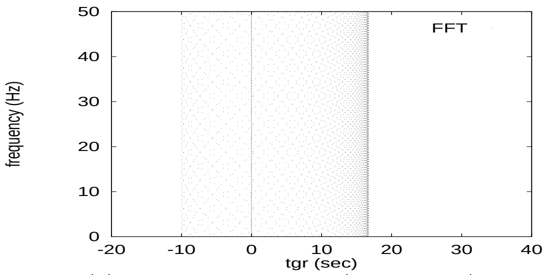

(c) Group delay time (Numerical)

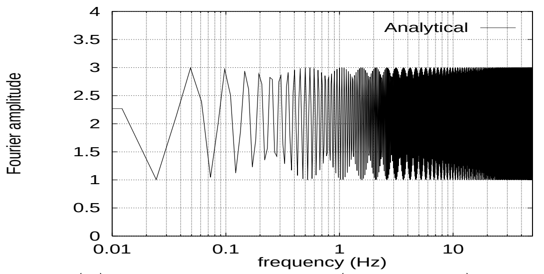

(d) Fourier amplitude (Analytical)

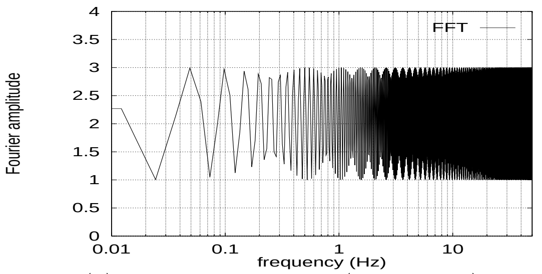

(e) Fourier amplitude (Numerical)

Figure 1 Comparison between analytical and numerical results for a impulse train with different magnitude.

Then, the mean and variance of X_n are $\mu_{X_n} = np$, $\sigma^2_{X_n} = np(1-p)$, respectively. Furthermore, the binomial variate X_n can be approximated by the normal variate with mean np and variance $np(1-p)$, provided $np(1-p) > 25$ for any p [Evans et al., 1993].

Now, let us consider $x(t_i)$ from Eq.(1) which represents the realized value of impulse train at a fixed time interval $[t_i, t_i + \Delta t]$, where Δt is a small increment of time. Then, $x(t_i)$ can be treated as Bernoulli trial. Applying the binomial distribution to the impulse train $x(t)$, n in Eq.(6) corresponds to the total number of impulses N, p to $f_T(t)\Delta t$, and X_n to n_i, where $f_T(t)$ is the probability density function of the occurrence time of impulses and n_i is the number of impulses occurred in a small time interval $[t_i, t_i + \Delta t]$. Since we will consider large N, n_i can be approximated by the normal variate for any t_i.

Thus, the stochastic impulse train $x(t)$ of Eq.(1) can be treated as Gaussian process represented by $N(\mu(t), \sigma^2(t))$, where the mean $\mu(t)$ and variance $\sigma^2(t)$ are, respectively,

$$\mu(t) = Np = Nf_T(t)\Delta t \tag{7}$$

$$\sigma^2(t) = Np(1-p) = Nf_T(t)\Delta t(1 - f_T(t)\Delta t). \tag{8}$$

To understand the characteristics of $x(t)$, we will divide $x(t)$ into two components: that is,

$$x(t) = x_m(t) + x_s(t), \tag{9}$$

where $x_m(t)$ is the trend process of $x(t)$ and $x_s(t)$ fluctuation from $x_s(t)$. From Eqs.(7) and (8), we can obtain

$$x_m(t) = Nf_T(t)\Delta t \tag{10}$$

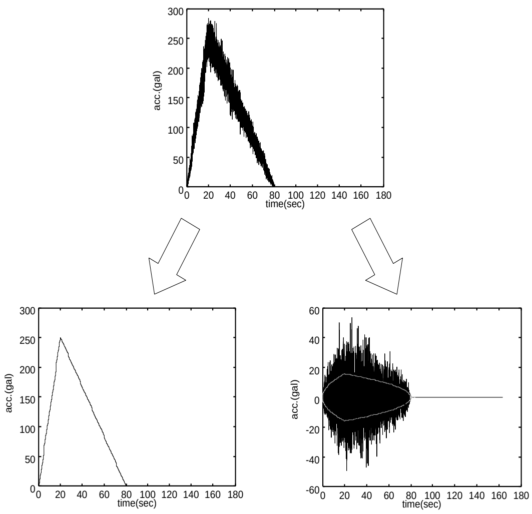

Figure 2 Schematic example for Eq.(9). upper panel: original impulse train $x(t)$, lower left panel: trend process $x_m(t)$, lower right panel: fluctuation $x_s(t)$.

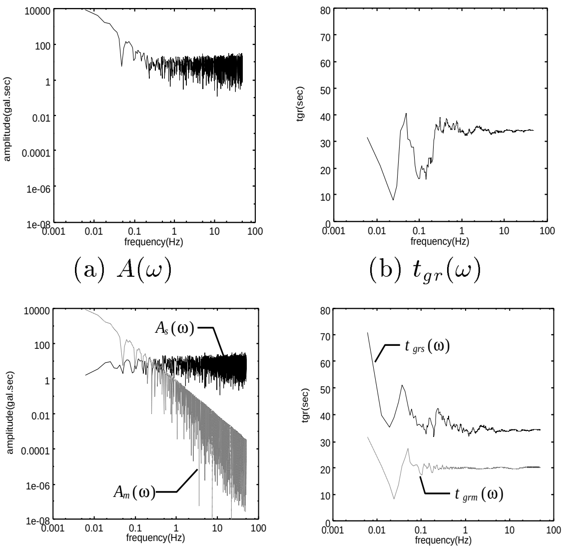

(c) $A_m(\omega)$ and $A_s(\omega)$ (d) $t_{grm}(\omega)$ and $t_{grs}(\omega)$

Figure 3 Fourier amplitude $A(\omega)$ and group delay time $t_{gr}(\omega)$

$$x_s(t) = N(0, Nf_T(t)\Delta t(1 - f_T(t)\Delta t)) = \sqrt{Nf_T(t)\Delta t(1 - f_T(t)\Delta t)} \cdot \xi(t), \tag{11}$$

where $\xi(t)$ is Gaussian process with zero-mean and the expectation $E[\xi(t_1)\xi(t_2)] = 0$ (as $t_1 \neq t_2$) or 1 (as $t_1 = t_2$).

Eq.(10) shows that the trend process $x_m(t)$ has similar shape with probability density function $f_T(t)$ for occurrence time of impulses. The coefficient in Eq.(11), that is, $\sqrt{Nf_T(t)\Delta t(1 - f_T(t)\Delta t)}$ can be regarded as the envelope function of $x_s(t)$. As an example, the trend process $x_m(t)$ and fluctuation $x_s(t)$ for a case where $f_T(t)$ is triangular distribution are shown in Figure 2.

3. FOURIER SPECTRUM OF IMPULSE TRAIN

3.1 Basic Properties

We will discuss the relationship between the stochastic process $x(t)$ and its components $x_m(t)$ and $x_s(t)$. It is considered that $x(t)$ is dominated by the component which has larger spectral amplitude. Namely, this can be formularized as

$$A(\omega) \simeq \begin{cases} A_m(\omega) & (\omega \leq \omega_c) \\ A_s(\omega) & (\omega \geq \omega_c) \end{cases} \tag{12}$$

$$t_{gr}(\omega) \simeq \begin{cases} t_{grm}(\omega) & (\omega \leq \omega_c) \\ pt_{grs}(\omega) & (\omega \geq \omega_c), \end{cases} \tag{13}$$

where $A(\omega)$, $A_m(\omega)$, and $A_s(\omega)$ stands for Fourier amplitude spectra, $t_{gr}(\omega)$, $t_{grm}(\omega)$, and $t_{grs}(\omega)$ for group delay time spectra for $x(t)$, $x_m(t)$, and $x_s(t)$, respectively. ω_c is a value on ω-axis for the intersection of $A_m(\omega)$ and $A_s(\omega)$. Although the group delay time spectrum has large fluctuation in high frequency range, our discussion, hereafter, will be focused on the average properties for simplicity.

$A(\omega)$, $A_m(\omega)$, and $A_s(\omega)$ are shown in the left panels of Figure 3 and $t_{gr}(\omega)$, $t_{grm}(\omega)$, and $t_{grs}(\omega)$ in the right panels. From this figure, Eq.(12) provides good approximation, while Eq.(13) cannot be acceptable because of the unsettled area in which the group delay time spectrum $t_{gr}(\omega)$ changes gradually from $t_{grm}(\omega)$ to $t_{grs}(\omega)$ around ω_c. One of reasons why such the area is observed, is existence of the fluctuation of $A_s(\omega)$ around ω_c. Because we cannot determine uniquely which Fourier amplitude of $x_m(t)$ and $x_s(t)$ is larger. We will call this area "transition area" and use ω^- and ω^+ as the frequencies at lower and upper boundary of the area, respectively. From Figure 3, it appears that $t_{gr}(\omega)$ changes linearly from $t_{grm}(\omega^-)$ to $t_{grs}(\omega^+)$ in the transition area. Figure 4 shows schematically the relationship between the Fourier amplitudes and group delay time spectra for $x(t)$, $x_m(t)$, and $x_s(t)$.

Dividing the frequency range into three parts, that is, low and high frequency and transition area, we will model $A(\omega)$ and $t_{gr}(\omega)$ for each frequency range in the following sections.

3.2 Low Frequency Range

Since the trend process $x_m(t)$ predominates in low frequency range, the Fourier spectrum can be determined without difficulty: that is,

$$A_m(\omega) = A_f(\omega) \cdot N\Delta t \tag{14}$$

$$t_{grm}(\omega) = t_{grf}(\omega), \tag{15}$$

where $A_f(\omega)$ and $t_{grf}(\omega)$ are Fourier amplitude and group delay time spectrum of $f_T(t)$, respectively.

In a case to multiply the number of impulses N by β, the value of $A_m(\omega)$ yields $\sqrt{\beta}$ times from Eq.(14). Furthermore, if $f_T(t)$ is triangular distribution, then $A_m(\omega)$ has gradient -2 on a log-log scale. Thus, the intersection ω_c of $A_m(\omega)$ and $A_s(\omega)$ is reduced to $\beta^{1/4}$ times.

3.3 High Frequency Range

On the other hand, fluctuation $x_s(t)$ predominates in high frequency range. Since $x_s(t)$ is Gaussian white noise multiplied by complicated envelope function as shown in Eq.(11), strict reduction of Fourier amplitude $A_s(\omega)$ and group delay time $t_{grs}(\omega)$ are generally difficult. We, therefore, will derive analytically the representative values of $A_s(\omega)$ and $t_{grs}(\omega)$.

For the Fourier amplitude $A_s(\omega)$ in high frequency range, it is considered that the average of $A_s(\omega)$ is constant from the observation of numerical results. The constant value coincides with the root mean squared of time series $x_s(t)$:

$$\begin{aligned} A_s(\omega) \equiv A_s &= \sqrt{\frac{1}{T}\int_0^T \{x_s(t)\}^2} = \sqrt{\frac{1}{T}\int_0^T \sigma^2(t)} \\ &= \sqrt{\frac{N}{T}\int_0^T f_T(t)(1 - f_T(t))dt}, \end{aligned} \tag{16}$$

where T denotes the duration time of $x(t)$.

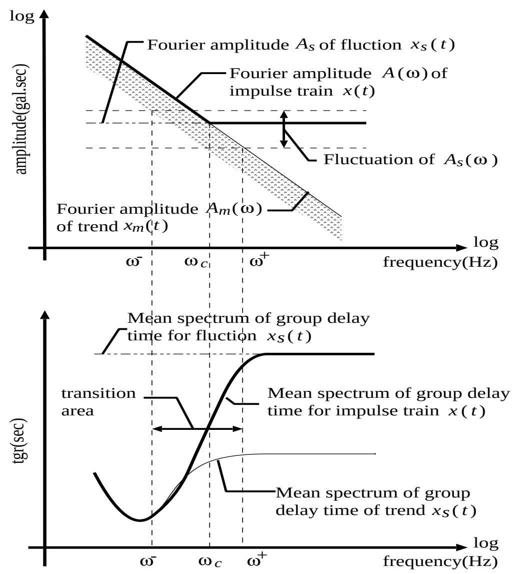

Figure 4 Relation between Fourier amplitude and group delay time of impulse train.

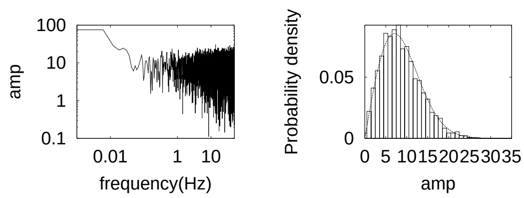

(a) Fourier amplitude (b) Histogram

Figure 5 PDF of Fourier amplitude.

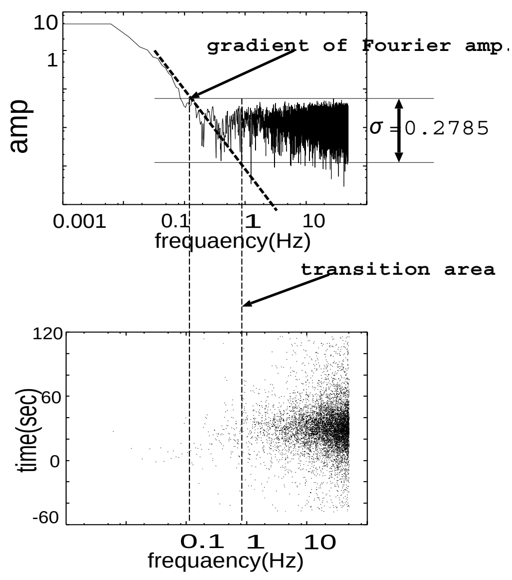

Figure 6 Determination of transition area.

Generally, the following relation can be obtained for any time series $z(t)$ [Izumi and Katsukura, 1983]:

$$\frac{1}{E}\int_{-\infty}^{\infty} t\cdot|\bar{z}(t)|^2 dt = \frac{1}{2\pi E}\int_{-\infty}^{\infty} t_{gr}(\omega)|\bar{Z}(\omega)|^2 d\omega, \tag{17}$$

where $\bar{z}(t)$ is the analytical function of $z(t)$, $\bar{Z}(\omega)$ the Fourier coefficients in complex of $\bar{z}(t)$, and

$$E = \int_{-\infty}^{\infty} |\bar{z}(t)|^2 dt = \frac{1}{2\pi}\int_{-\infty}^{\infty} |\bar{Z}(\omega)|^2 d\omega. \tag{18}$$

Eq.(17) means that the center of gravity for squared envelope function $|\bar{z}(t)|^2$ coincides with average of group delay time spectrum.

For the group delay time spectrum $t_{grs}(\omega)$ in high frequency range, it seems that the average of $t_{grs}(\omega)$ is constant, and then we will use t_{grs} as such the constant value. Taking Eq.(17) into account, t_{grs} yields

$$t_{grs} = \frac{1}{E}\int_0^T t\sigma^2(t)dt = \frac{1}{E}\int_0^T t\cdot Nf_T(t)(1-f_T(t))dt, \tag{19}$$

where

$$E = \int_0^T \sigma^2(t)dt = \int_0^T Nf_T(t)(1-f_T(t))dt. \tag{20}$$

3.4 Transition Area

To determine the lower and upper boundary of transition area ω^- and ω^+ for $t_{gr}(\omega)$, we have to analytically estimate the variance of $A(\omega)$ in high frequency range. If t_k $(k = 1, 2, \ldots, N)$ are random variables in Eq.(1), the probability density function of $x = A(\omega)$ is derived from Eq.(3) for large N as follows:

$$f_A(x) = \frac{2x}{N}\exp\left(-\frac{x^2}{N}\right). \tag{21}$$

It should be notice in this equation that $f_A(x)$ is independent of the probability density function $f_T(t)$ for the occurrence time of impulses. In Figure 5, Eq.(21) is compared with a histogram of Fourier amplitude which is obtained from numerically simulated impulse train $x(t)$ of Eq.(1). From this figure, it is observed that Eq.(21) agrees with the numerical result.

Using relation $y = \log x$, moreover, Eq.(21) is transformed as

$$f_Y(y) = \frac{2\ln 10\cdot 10^{2y}}{n}\cdot\exp\left(-\frac{10^{2y}}{n}\right). \tag{22}$$

Then, the mean μ_y and standard deviation σ_y of the random variable y are

$$\mu_y = -\frac{1}{2\ln 10}\left(\mathcal{C} + \ln\frac{1}{n}\right) \tag{23}$$

$$\sigma_y = \ln 10\sqrt{\frac{\pi}{24}} = 0.2785, \tag{24}$$

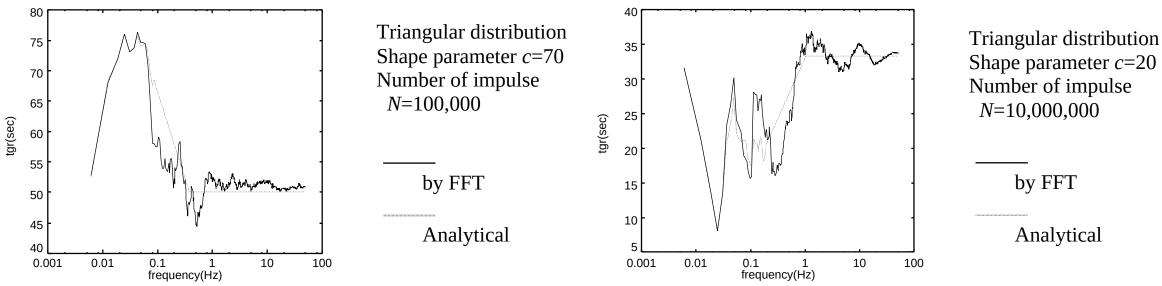

Figure 7 Example of the estimated group delay time.

where $\mathcal{C}$ stands for Euler's constant. From Eq.(24), the standard deviation of $\log A(\omega)$ is constant: namely, it is independent of number of impulses N and PDF $f_T(t)$ for occurrence time of impulses. This means that the range of transition area depend only on the gradient of Fourier amplitude of trend process $x_m(t)$. Using the properties obtained above, we can determine the transition area as shown in Figure 6.

4. MODELING PHASE SPECTRA

On the basis of the discussion in the previous sections, we can determine the spectral properties of source time function modeled by stochastic impulse train. The procedure for modeling the spectrum is given as follows:

(1) $x(t)$ is divided into two components: that is, $x(t) = x_m(t) + x_s(t)$, where $x_m(t)$ stands for trend and $x_s(t)$ for fluctuation.

(2) $x_m(t)$ and $x_s(t)$ are represented by

$$x_m(t) = N f_T(t)\Delta t \tag{25}$$

$$x_s(t) = \sqrt{N f_T(t)\Delta t(1 - f_T(t)\Delta t)} \cdot \xi(t), \tag{26}$$

where $\xi(t)$ is Gaussian process with zero-mean and expectation $E[\xi(t_1)\xi(t_2)] = 1$ (as $t_1 = t_2$) or 0 (as $t_1 \neq t_2$).

(3) Fourier amplitude and group delay time for $x_m(t)$ are obtained through the Fourier transform of $f_T(t)$:

$$A_m(\omega) = A_f(\omega) \cdot N\Delta t \tag{27}$$

$$t_{grm}(\omega) = t_{grf}(\omega). \tag{28}$$

(4) Fourier amplitude of $x_s(t)$ is calculated as root mean squared of envelope function for $x_s(t)$:

$$A_s = \sqrt{\frac{N}{T}\int_0^T f_T(t)(1 - f_T(t))dt}. \tag{29}$$

(5) Group delay time of $x_s(t)$ is calculated as the center of gravity of envelope function for $x_s(t)$:

$$t_{grs} = \frac{1}{E}\int_0^T t \cdot N f_T(t)(1 - f_T(t))dt. \tag{30}$$

(6) Then, $A(\omega)$ is obtained as follows:

$$A(\omega) \simeq \begin{cases} A_m(\omega) = A_f(\omega) \cdot N\Delta t & (\omega \leq \omega_c) \\ A_s \quad\;\; = \sqrt{\frac{N}{T}\int_0^T f_T(t)(1 - f_T(t))dt} & (\omega > \omega_c). \end{cases} \tag{31}$$

(7) The standard deviation of $\log A_s(\omega)$ is independent of N and $f_T(t)$: $\sigma_{A_s} = 0.2785$.

(8) The lower and upper boundaries of transition area ω^- and ω^+ are determined from σ_{A_s} and $A_m(\omega)$.

(9) Then, $t_{gr}(\omega)$ is obtained as follows:

$$t_{gr}(\omega) \simeq \begin{cases} t_{grm}(\omega) = t_{grf}(\omega) & (\omega < \omega^-) \\ t_{grm}(\omega^-) + \dfrac{\log\omega - \log\omega^-}{\log\omega^+ - \log\omega^-}\{t_{grs}(\omega^+) - t_{grm}(\omega^-)\} & (\omega^- \leq \omega < \omega^+) \\ t_{grs} = \frac{1}{E}\int_0^T t \cdot N f_T(t)(1 - f_T(t))dt & (\omega^+ \leq \omega). \end{cases} \tag{32}$$

The average properties of group delay time for impulse train is uniquely determined from only two factors, namely, the number of impulses N and the probability density function $f_T(t)$ for occurrence time of impulses. Figure 7 shows $t_{gr}(\omega)$ estimated on the basis of $f_T(t)$ and N following the above procedure. In this figure, it is observed that the analytically obtained $t_{gr}(\omega)$ agrees with the result calculated by FFT method. This means that the proposed method is appropriate for analysis of phase properties of source time function.

6. CONCLUSIONS

The conclusions derived from this study are summarized as follows:

1. The stochastic impulse train can be divided into two components such as trend process and fluctuation from trend. Then, the spectral properties of impulse train are dominated by a component which has larger spectral amplitude.
2. The spectral properties of source time function depend on the trend process in low frequency range and on the fluctuation from trend in high frequency range.
3. In the middle frequency range, the "transition area" appears because of the fluctuation of Fourier amplitude. The range of transition area can be determined by the standard deviation of Fourier amplitude in high frequency range, which is constant and independent of number of impulses and PDF for occurrence time of impulses.
4. It is shown that we can analytically derive the average properties for group delay time spectrum of impulse train using only two factors which are the number of impulses and PDF for occurrence time of impulses.

REFERENCES

Evans, M., Hastings, N., and Peacock, B. (1993), *Statistical Distribution*, Second Edition, Johon Wiley & Sons, New York, pp.38–41.

Daley, D.J. and Vere-Jones, D. (1988), *An Introduction to the Theory of Point Processes*, Springer-Verlag, New York.

Izumi, M. and Katsukura, Y. (1983), "A Fundamental Study on Extraction of Phase Information in Earthquake Motions," *J. Struct. Constr. Eng.*, AIJ, No. 327, pp.20–27 (in Japanese).

Lin, Y.K. and Cai, G.Q. (1995), *Probabilistic Structural Dynamics*, McGraw-Hill, pp.41–47.

Ohsaki, Y. (1979), "On the Significance of Phase Content in Earthquake Ground Motions," *Earthquake Engineering and Structural Dynamics*, Vol. 7, pp.427–439.

Soda, S. (1986), "Basic Study on Application of Probability Characteristics of Phase Inclination to Non-stationary Random Vibration Analysis," *J. Struct. Constr. Eng.*, AIJ, No. 365, pp.48–57 (in Japanese).

Vanmarcke, E. (1983), *Random Fields*, MIT press, Massachusetts, pp.91–92.